Journal of Inorganic and General Chemistry
ZAAC
Zeitschrift für anorganische und allgemeine Chemie
DOI: 10.1002/zaac.201800140
ARTICLE

Synthetic Access to Derivatized Mn-Pyane as a Redox-modulated Pool of SODm

Andreas Scheitler,[a] Felix Friedel,[a] Ralph Puchta,[a,b] Carlos Dücker-Benfer,[a] and Ivana Ivanović-Burmazović*[a]

Dedicated to Prof. Peter Comba on the Occasion of his 65th Birthday

Abstract. In this work, four derivatives of the pentaazamacrocyclic Mn-pyane [pyane = *trans*-2,13-dimethyl-3,6,9,12,18-pentaazabicyclo[12.3.1]-octadeca-1(18),14,16-triene] complex were synthesized and characterized, carrying small substituents at the pyridine ring that allow fine-tuning of the manganese centered redox potential, without significant change to the overall complex arrangement that is crucial for a correct comparison regarding their superoxide dismutase mimetic (SODm) capabilities. The crystal structure of the seven-coordinate OMe-substituted Mn-pyane complex was obtained. The synthesized complexes will serve for future investigations related to an effect of complex redox potentials on their mechanistic behavior within SOD catalysis.

Introduction

One of the roots of supramolecular chemistry is the serendipitous synthesis of crown ether, especially dibenzo[18]crown-6, by *Charles J. Pedersen*. His publication in 1967 summarised an extensive study on preparation and their inclusion complexes.[1] This outstanding work was awarded by the noble prize in 1987 together with *D. Cram* and *J.-M. Lehn*.[2] *Atkins* et al. later extended the crown ethers to their aza analogues.[3] Due to the biological relevance of N-donors these compounds were immediately applied in biomimetic chemistry. In this report we want to design a new potential superoxide dismutases mimetics (SODm) utilizing the well known pentaazamacrocyclic motif of pyane [*trans*-2,13-dimethyl-3,6,9,12,18-pentaazabicyclo[12.3.1]-octadeca-1(18),14,16-triene] ligand that belongs to aza analogues of crown ethers.

The superoxide radical anion $O_2^{\bullet-}$ is the product of a formal one electron reduction from molecular oxygen and is a key role player in the group of reactive oxygen species (ROS). The overexpression of ROS in the human body is what we call oxidative stress, and is as we know today one of the main issues regarding a catalogue of diseases as well as chronic pain issues and cancer.[4] Superoxide is generated in large quantities, namely up to 3% of consumed oxygen, in the mitochondria as a by-product of cellular respiration.[5] To enable superoxide regulation there is a class of metalloenzymes, called superoxide dismutases (SOD), which scavenge superoxide to form oxygen and hydrogen peroxide at rates near the diffusion limit.

A lot of work has been published over the last decades, developing small artificial molecules that mimic the functionality of native SOD enzymes and could therefore be used as therapeutics for diseases originating from superoxide overexpression. Most of those SOD mimics contain manganese, iron, copper, and/or zinc, just like the native enzymes, with manganese being more potent and less toxic than a lot of copper and iron based SODm. Although a vast amount of SOD mimics have been synthesized and published over the last decades, most of them were assayed by indirect methods, like the cytochrome *c* assay,[6] the NBT assay,[7] or similar methods that rely on small steady state concentrations of superoxide and some form of indicator molecule for spectroscopic observation.

These kinds of indirect assays for determination of SOD activity, for any potential SOD mimic, are intrinsically flawed since cross reactions between SODm intermediates during catalysis and indicator molecules or other components of the respective assay are never to be ruled out. This kind of side reactions often lead to misinterpretations regarding the catalytic rate constant that is determined to compare the potency of SOD mimics. Unfortunately, the errors are not limited to an over- or underestimation of the given results, but can lead to a false positive that allows for catalytic inactive compounds to be misjudged for active SOD mimics. Using the results of the commonly used, indirect assays, a lot of work has been published comparing SOD mimics, claiming links between complex redox-potential, steric accessibility of active sites, and superiority of some classes over others[8]. While these comparisons are valuable, the data used to make these rankings are usually questionable. Furthermore it is common practice to postulate mechanisms for SOD catalysis by any given new

* Dr. I. Ivanović-Burmazović
E-Mail: ivana.ivanovic-burmazovic@fau.de
[a] Department of Chemistry and Pharmacy
Friedrich-Alexander University Erlangen-Nürnberg
Egerlandstrasse 1
91058 Erlangen, Germany
[b] Central Instituite for Scientific Computing (ZISC)
Friedrich-Alexander University Erlangen-Nürnberg
Martensstrasse 5a
91058 Erlangen, Germany

compound, but relying on indirect assays, consistent interpretations are difficult to obtain.

Since we know that SOD catalysis is a very delicate field of research, that requires great attention to detail, especially when it comes to mechanistic assertions. We synthesized derivatives of a very well-studied, proven SOD mimic, Mn-pyane, carrying small substituents that allow redox fine tuning of the central manganese metal atoms, without influencing any steric demands surrounding the immediate environment of the active site of SOD catalysis. These compounds will serve for future detailed mechanistic investigations based on a direct method for quantification of SOD activity[9].

Experimental Section

Materials and Instruments: Reagents and solvents were obtained by commercial sources and were of high purity. Carlo Erba elemental analyzers 1106 and 1108 were used for chemical analysis. NMR spectra were recorded with a Bruker AVANCE DRX400 WB. A Bruker Daltonics (Bremen, Germany) maXis™ UHR-ToF mass spectrometer was used for ESI-ToF measurements. Detection was in positive-ion mode, the source voltage was adjusted for every measurement. The flow rate was 180 μL·h^{-1} and the drying gas (N_2) was held at 180 °C for standard measurements. The machine was calibrated prior to every experiment by direct infusion of either an Agilent ESI-ToF low concentration tuning mixture or commercial lithium-formate solution. Ligand syntheses were carried out under ambient air conditions unless stated otherwise, complex syntheses were performed in a nitrogen atmosphere using standard Schlenk techniques. X-ray data collection for the structure determinations were carried out with a Rigaku Oxford Diffraction (formerly Agilent) Supernova A S2 (Dual) Diffractometer using an Atlas S2 CCD detector and Nova (Cu, Cu-K_α: λ = 1.54184 Å) X-ray Source. The crystals were coated with perfluoropolyether, picked with a glass fiber or a loop, and immediately mounted in the nitrogen cold gas stream of the diffractometer. The images were interpreted and integrated with the program CrysAlisPro (Agilent Technologies)[10]. The structures were solved by using direct methods and refined with full-matrix least-squares against F^2 (SHELXS/SHELXT[11] as part of Olex2[12]). A weighting scheme was applied in the last steps of the refinement with $\omega = 1/[\sigma^2 (F_0^2 + (aP)^2 + bP]$ and $P = [2F_c^2 + \max(F_0^2, 0)]/3$. Non-hydrogen atoms were anisotropically refined and hydrogen atoms were included in their calculated positions and refined in a riding model. The structure pictures were prepared with the program Mercury.[13]

General Procedure for the Synthesis of R-DAP (DAP = 1,1′-(2,6-Pyridinediyl)diethanone):[14] 4-substituted pyridine (1.0 equiv.) was dissolved in aqueous sulfuric acid (0.4 M, 5 mL per mmol of R-pyridine). Pyruvic acid (3.5 equiv.) and $AgNO_3$ (0.025 equiv.) were added to the solution. Small amounts of $(NH_4)S_2O_8$ were added and additional $AgNO_3$ was added to start the reaction if necessary. The remaining $(NH_4)_2S_2O_8$ (4.0 equiv.) was added in small portions and the reaction solution was stirred for at least 18 h at room temperature. The brownish solution was extracted with dichloromethane (3 × 100 mL). The extract was dried ($MgSO_4$) and the solvent was removed by rotary evaporation to yield the crude product. The desired R-DAP was isolated by column chromatography.

4-Chloro-DAP (1): Cl-DAP was synthesized starting from 4-chloropyridine hydrochloride (7.50 g, 50.3 mmol), which was dissolved in H_2O (50 mL) and neutralized by addition of Na_2CO_3. 4-Chloropyridine was extracted by dichloromethane (3 × 50 mL), which was removed under reduced pressure after drying over $MgSO_4$. The resulting orange oil was used without further purification in the standard procedure for the synthesis of R-DAP, described above. Cl-DAP was isolated after purification by column chromatography (SiO_2, dichloromethane, R_f = 0.63) as a colorless, crystalline solid (856 mg, 4.34 mmol, 10 %). **^{1}H NMR** (400 MHz, $CDCl_3$, 25 °C): δ = 2.78 (s, 6 H, COCH_3), 8.18 (s, 2 H, Ar*H*). **^{13}C NMR** (100 MHz, $CDCl_3$, 25 °C): δ = 25.6, 124.9, 146.9, 153.9, 198.1 ppm. **IR**: $\tilde{\nu}$ = 3080 m, 2926 w, 1705 s, 1568 s, 1408 m, 1360 s, 1304 s, 1223 s, 1125 s, 903 s, 808 s cm^{-1}. $C_9H_8ClNO_2$: calcd.C 54.70; H 4.08; N 7.09 %; found: C 55.00; H 3.89; N 6.57 %.

4-Cyano-DAP (2): The synthesis of CN-DAP was carried out using the standard procedure described above. Crude **2** was purified by a short silica plug (dichloromethane) followed by recrystallization from EtOAc/hexane. CN-DAP was isolated as a colorless crystalline solid (1.64 g, 8.72 mmol, 13 %). **^{1}H NMR** (300 MHz, $CDCl_3$, 25 °C): δ = 2.81 (s, 6 H, COCH_3), 8.40 (s, 2 H, Ar*H*). **^{13}C NMR** (75 MHz, $CDCl_3$, 25 °C): δ = 25.5, 115.4, 123.1, 126.2, 153.6, 197.3. **IR**: $\tilde{\nu}$ = 3092 m, 2932 w, 2245 w, 1697 s, 1589 m, 1366 s, 1231 s, 1171 s, 912 s, 866 m cm^{-1}. $C_{10}H_8N_2O_2$: calcd. C 63.83; H 4.29; N 14.89 %; found: C 63.92; H 3.82; N 13.98 %.

4-Trifluoromethyl-DAP (3): CF_3-DAP was synthesized following the standard procedure for the acetylation of R-pyridines. **3** was isolated by column chromatography (SiO_2, dichloromethane, R_f = 0.65) as a colorless, crystalline solid (1.31 g, 5.66 mmol, 42 %). **^{1}H NMR** (400 MHz, $CDCl_3$, 25 °C): δ = 2.83 (s, 6 H, COCH_3), 8.43 (s, 2 H, Ar*H*). **^{13}C NMR** (100 MHz, $CDCl_3$, 25 °C): δ = 25.5, 120.5, 140.9, 153.9, 197.8 ppm. $C_{10}H_8F_3NO_2$: calcd. C 51.96; H 3.49; N 6.06 %; found: C 52.19; H 2.99; N 6.02 %. **IR**: $\tilde{\nu}$ = 3096 w, 3013 w, 1703 s, 1422 m, 1348 s, 1254 s, 1233 s, 1132 s cm^{-1}.

4-Methylcarboxy-DAP (4): 4 was synthesized as described above and purified by column chromatography (SiO_2, dichloromethane, R_f = 0.67). CO_2Me-DAP **4** was isolated as a colorless crystalline solid (930 mg, 4.21 mmol, 11 %). **^{1}H NMR** (300 MHz, $CDCl_3$, 25 °C): δ = 2.81 (s, 6 H, COCH_3), 4.00 (s, 3 H, CO_2CH_3), 8.73 (s, 2 H, Ar*H*). **^{13}C NMR** (75 MHz, $CDCl_3$, 25 °C): δ = 25.7, 68.1, 124.0, 140.1, 153.8, 164.4, 168.2, 198.4 ppm. IR: $\tilde{\nu}$ = 3094 w, 2967 w, 1726 s, 1699 s, 1560 w, 1433 m, 1362 m, 1244 s, 949 s, 770 s cm^{-1}. $C_{11}H_{11}NO_4$: C 59.73; H 5.01; N 6.33 %; found: C 59.87; H 4.73; N 5.85 %.

4-Chloro-2,6-bis[2-methyl-(1,3-dioxolan-2-yl)]-pyridine[15] (5): To a solution of **1** (2.00 g, 10.1 mmol) in toluene (100 mL), *p*-toluenesulfonic acid (111 mg, 643 μmol) and 1,2-ethylene glycol were added. The reaction mixture was refluxed for 21 h as water was separated from the solution. After cooling, the solvent was removed and a yellow oil remained. The residue was dissolved in dichloromethane (50 mL) and was washed with a 5 % $KHCO_3$ solution. The aqueous phase was extracted with dichloromethane (3 × 20 mL). The combined organic extracts were dried with Na_2SO_4 and the solvent was removed under reduced pressure. The residual yellow oil was purified by a short silica plug (dichloromethane/EtOAc; 5/2) and yielded **5** as a yellowish oil (2.60 g, 9.12 mmol, 90 %). **^{1}H NMR** (300 MHz, $CDCl_3$, 25 °C): δ = 1.74 (s, 6 H, COCH_3), 3.93 (m, 4 H, OCH_2CH_2O), 4.10 (m, 4 H, OCH_2CH_2O), 7.49 (s, 2 H, Ar*H*). **^{13}C NMR** (75 MHz, $CDCl_3$, 25 °C): δ = 24.6, 65.1, 82.8, 108.3, 119.2, 145.1, 162.2 ppm.

4-Methoxy-2,6-bis[(2-methyl-(1,3-dioxolan-2-yl)]-pyridine[16] (6): Elemental sodium (0.250 g, 10.9 mmol) was dissolved in abs. MeOH (15 mL) in an inert atmosphere (N_2). **5** (2.60 g, 9.10 mmol, suspended in 30 mL abs. MeOH) was added to the solution. The yellow reaction

mixture was refluxed for 24 h and additional sodium methoxide solution (35 mL) was added. After refluxing for 3 d, the orange reaction mixture was cooled to room temperature and the precipitate was filtered off. The filtrate was concentrated in vacuo and ice water was added. The aqueous phase was extracted with dichloromethane (3 × 50 mL), the combined organic residues were dried with $MgSO_4$ and the solvent was removed. **6** was isolated as an orange oil. (2.49 g, 8.86 mmol, 97 %). **^{1}H NMR** (400 MHz, $CDCl_3$, 25 °C): δ = 1.72 (s, 6 H, $COCH_3$), 3.84 (s, 3 H, OCH_3), 3.90 (t, 4 H, OCH_2CH_2O, J = 8.0 HHHHz), 4.06 (t, 4 H, OCH_2CH_2O, J = 8.0 Hz), 6.99 (s, 2 H, Ar*H*). **^{13}C NMR** (100 MHz, $CDCl_3$, 25 °C): δ = 24.6, 55.1, 64.9, 104.5, 108.5, 162.2, 166.7 ppm.

4-Methoxy-DAP[17] (7): **6** (1.64 g, 5.83 mmol) was dissolved in THF (100 mL) and conc. $HClO_4$ (9.5 mL) was added. The solution was refluxed for 2 h and the color turned from yellow to orange. The solvent was removed and the oily residue was neutralized by addition of saturated Na_2CO_3 solution. The yellowish solution was extracted with dichloromethane (4 × 20 mL) and Et_2O (2 × 20 mL). The organic phases were combined and dried with $MgSO_4$. The solvent was removed to yield the crude as an orange solid, which was purified by a silica plug (dichloromethane, R_f = 0.45). OMe-DAP **7** was isolated as a colorless crystalline solid (442 mg, 2.30 mmol, 39 %). **^{1}H NMR** (400 MHz, $CDCl_3$, 25 °C): δ = 2.76 (s, 6 H, $COCH_3$), 3.94 (s, 3 H, OCH_3), 7.69 (s, 2 H, Ar*H*). **^{13}C NMR** (100 MHz, $CDCl_3$, 25 °C): δ = 25.7, 55.9, 110.5, 154.6, 167.5, 199.4 ppm. **IR**: $\tilde{\nu}$ = 3088 m, 2959 w, 1692 s, 1589 s, 1410 m, 1360 s, 1229 m, 1042 s, 878 s. $C_{10}H_{11}NO_3$: calcd. C 62.17; H 5.74; N 7.25 %; found: C 62.34; H 5.26; N 6.56. %

General Procedure for the Synthesis of Mn-R-pyane[18]: To a solution of R-DAP (1.0 equiv.) in abs. MeOH (15 mL per mmol R-DAP) $MnCl_2{\cdot}2H_2O$ (1 equiv.) was added. Triethylenetetramin (1 equiv.) was diluted in abs. MeOH (10 mL) and the solution was added to the reaction mixture over a period of 10 min. The solution was refluxed for 2 h while the color turned red. After cooling to room temp. $NaBH_4$ (4 equiv. per double bond) was added. The solution was stirred overnight at room temperature and refluxed for 3 h the next day, when the color changed to a pale yellow. Solid LiCl (10 equiv.) was added and stirring continued for 30 min at room temperature. The solvent was removed by rotary evaporation and the solid, brownish residue was dissolved in as less millipore water as possible. The aqueous solution was extracted with dichloromethane (3 × 100 mL). The combined organic layers were dried with $MgSO_4$ and the solvent was removed, which yielded Mn-R-pyane. Crystallization and purification was achieved by slow ether diffusion in a conc. methanolic Mn-R-pyane solution.

[Mn(Cl-pyane)(Cl)$_2$] (8): **1** (400 mg, 2.03 mmol), $MnCl_2{\cdot}2H_2O$ (327 mg, 2.03 mmol), triethylenetetramine (0.30 mL, 2.03 mmol), $NaBH_4$ (618 mg, 16.3 mmol). **8** was obtained as a yellow powder (802 mg, 1.84 mmol, 90 %). **UHR-MS** (ESI, MeOH, *m/z*): 383.1284 $[M - 2\,Cl + OH]^+$ (383.1279 calcd. for $C_{15}H_{26}ClMnN_5OH$), 401.0951 $[M - Cl]^+$ (401.0940 calcd. for $C_{15}H_{26}Cl_2MnN_5$). $C_{15}H_{26}Cl_3MnN_5$: calcd. C 41.16; H 5.99; N 16.00 %; found: C 41.00; H 6.13; N 15.68 %. **IR**: $\tilde{\nu}$ = 3227 m, 2907 m, 2859 m, 1582 s, 1119 s, 891 s, 814 s cm^{-1}.

[Mn(CH$_2$NH$_2$-pyane)(Cl)$_2$] (9): **2** (1.00 g, 5.32 mmol), $MnCl_2{\cdot}2H_2O$ (856 mg, 5.32 mmol), triethylenetetramine (0.79 mL, 5.32 mmol), $NaBH_4$ (3.24 g, 85.1 mmol). **9** was obtained as a yellow powder (902 mg, 2.09 mmol, 39 %). **UHR-MS** (ESI, MeOH, *m/z*): 180.5989 $[M - 2\,Cl]^{2+}$ (180.5951 calcd. for $C_{16}H_{30}MnN_6$), 396.1657 $[M - Cl]^+$ (396.1595 calcd. for $C_{16}H_{30}ClMnN_6$). $C_{16}H_{30}Cl_2N_6Mn + 1/2CH_2Cl_2$: calcd. C 41.74; H 6.58; N 17.70 %; found: C 41.16; H 6.67; N 16.28 %. **IR**: $\tilde{\nu}$ = 3208 s, 2911 m, 2862 m, 1613 s, 1451 s, 1123 s, 810 s cm^{-1}.

[Mn(CF$_3$-pyane)(Cl)$_2$] (10): **3** (1.39 g, 6.02 mmol), $MnCl_2{\cdot}2H_2O$ (969 mg, 6.02 mmol), triethylenetetramine (0.90 mL, 6.02 mmol), $NaBH_4$ (1.83 g, 48.2 mmol). **10** was obtained as an orange solid (1.36 g, 2.89 mmol, 48 %). **UHR-MS** (ESI, MeOH, *m/z*): 417.1536 $[M - 2\,Cl + OH]^+$ (417.1543 calcd. for $C_{16}H_{27}F_3MnN_5O$). $C_{16}H_{26}Cl_2F_3MnN_5$: calcd. C 40.78; H 5.56; N 14.86 %; found: C 40.48; H 5.19; N 14.38 %. **IR**: $\tilde{\nu}$ = 3227 m, 2907 m, 2861 m, 1578 m, 1136 s, 810 s cm^{-1}.

[Mn(OMe-pyane)(Cl)$_2$] (11): **7** (355 mg, 1.85 mmol), $MnCl_2{\cdot}2H_2O$ (298 mg, 1.85 mmol), triethylenetetramine (0.27 mL, 1.85 mmol), $NaBH_4$ (560 mg, 14.8 mmol). **11** was obtained as a beige powder (706 mg, 1.63 mmol, 88 %). **UHR-MS** (ESI, MeOH, *m/z*): 379.1781 $[M - 2\,Cl + OH]^+$ (379.1774 calcd. for $C_{16}H_{29}OMnN_5OH$), 397.1444 $[M - Cl]^+$ (397.1436 calcd. for $C_{16}H_{29}ClMnN_5$). $C_{16}H_{29}Cl_2N_5MnO + CH_3OH$: calcd. C 43.88; H 7.15; N 15.05 %; found: C 43.10; H 6.60; N 14.99 %. **IR**: $\tilde{\nu}$ = 3244 m, 2916 m, 2862 m, 1607 s, 1570 s, 1447 s, 1341 s, 1121 s, 1038 s cm^{-1}.

CCDC 1850316 contains the supplementary crystallographic data for this paper. These data can be obtained free of charge via www.ccdc.cam.ac.uk/data_request/cif, or by emailing data_request@ccdc.cam.ac.uk, or by contacting The Cambridge Crystallographic Data Centre, 12 Union Road, Cambridge CB2 1EZ, UK; fax: +44 1223 336033.

Results and Discussion

Syntheses

Mn^{II}-R-pyane complexes were synthesized by introducing both, electron donating and electron withdrawing substituents to the 4-position of the 2,6-diacetylpyridine (DAP) precursor. In case of electron withdrawing groups, a synthesis by *Zong*, et al.[14] starting from 4-substituted pyridine was used to obtain 4-R-DAP in low yields of around 10 % (Figure 1). With CF_3 being the most electron withdrawing group that was introduced to the ligand, acetylation by this radical based synthesis worked best with a yield of 42 %.

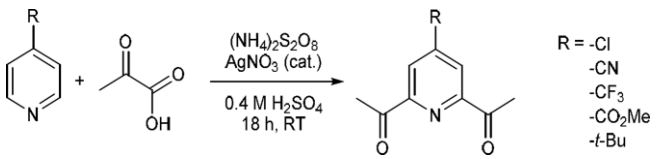

Figure 1. Synthesis of R-DAP by *Zong* et al.[14]

Acetylation following this procedure is not a suitable method for pyridines carrying electron donating groups at the 4-position. The methoxy (OMe) substituent was introduced by a series of reactions starting from 4-chloro-DAP **1**. First, the acetyl groups were transformed into acetals by reaction with ethylene glycol. Reaction with in situ generated sodium methoxide followed by removal of the protecting groups gave 4-methoxy-DAP **7** (Figure 2).

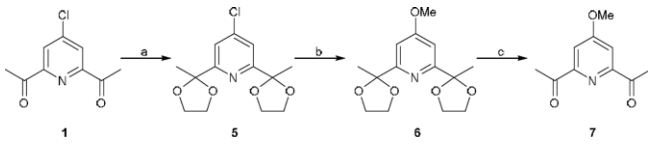

Figure 2. Synthesis of OMe-DAP[15–17]. (a) *p*-toluenesulfonic acid, 1,2-ethylene glycol, toluene, reflux 21 h. (b) Na, MeOH, reflux 23 h. (c) $HClO_4$, THF, reflux 2 h.

$[Mn^{II}(R\text{-pyane})(Cl)_2]$ complexes were synthesized in a one-pot, two-step synthesis from the respective R-DAP precursors (Figure 3).

The respective R-DAP and manganese chloride were dissolved in methanol to form a pre-coordinated Mn-R-DAP species. Using Mn^{II} as a template, triethylenetetramine was added to form the pentaazamacrocycle by condensation reaction. The $[Mn^{II}(R\text{-pydiene})(Cl)_2]$ complexes were not isolated, but in situ transformed, in a second step, to their $[Mn^{II}(R\text{-pyane})(Cl)_2]$ analogues, by hydrogenation of the imine bonds to secondary amine functionalities by homogeneous reduction with sodium borohydride. For the $[Mn^{II}(OMe\text{-pyane})(Cl)_2]$ complex it was possible to grow crystals suitable for X-ray analysis by slow diffusion of ethyl ether into a concentrated methanolic complex solution over a period of two weeks. The synthetic method described above was successfully performed for R = –Cl (**8**), $–CH_2NH_2$ (**9**) (result of the reduction of the –CN functionality), $–CF_3$ (**10**), and –OMe (**11**). In the case of R = $–CO_2Me$ the respective pyane complex was not isolated. ESI-MS data indicated that the ester group was reacting in the presence of sodium borohydride, yielding a variety of reduction products, i.e. –CHO, $–CH_2OH$ and $–CH_3$, which is quite unusual considering the well-established inertness of methylesters vs. sodium borohydride. We assume that coordination of the pyridine-*N* to manganese metal center shifts electron density to such an extent that sodium borohydride is a strong enough reductant to enable reactions with the ester functionality.

Crystal Structure of $[Mn^{II}(H\text{-pyane})(Cl)_2]$

A selection of bond lengths and bond angles for $[Mn^{II}(OMe\text{-pyane})(Cl)_2]$ are shown in Table 1. The corresponding values are also compared to those of the previously published, unsubstituted $[Mn^{II}(H\text{-pyane})(Cl)_2]$ complex[19].

The structure of the complex shown in Figure 4 is quite similar to the structure reported of unsubstituted $[Mn^{II}(H\text{-pyane})(H_2O)_2]$[19]. Introduction of a small functional group does not seem to affect the geometry of the complex, which is important when the effect of the metal centered redox potential is investigated in regard to SOD activity. The complex has a pentagonal-bipyramidal (PBP) structure, which is centered on the manganese(II) ion. The neutral OMe-pyane ligand occupies the

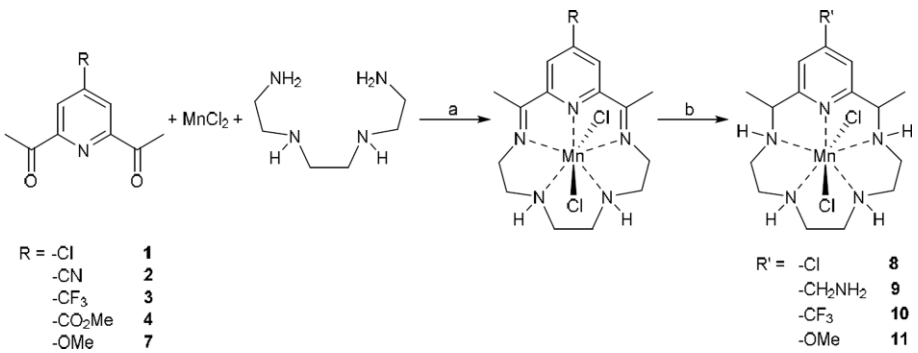

Figure 3. Synthesis of Mn-R-pyane. (a) MeOH, reflux 2 h. (b) $NaBH_4$, MeOH, reflux 3 h.

Table 1. Selected bond lengths /Å and bond angles /° of $[Mn^{II}(H\text{-pyane})(H_2O)_2]$ and $[Mn^{II}(OMe\text{-pyane})(Cl)_2]$.

Bond	Bond length	Literature value Mn-H-pyane [19]	Bond	Bond length
Mn1–Cl1	2.5844(7)	2.282(3) [a]	N2-C7	1.475(3)
Mn1–Cl2	2.5927(7)	2.241(3) [a]	N2-C9	1.474(3)
Mn1–N1	2.293(2)	2.278(3)	N5-C14	1.473(3)
Mn1–N2	2.345(2)	2.343(3)	N5-C15	1.468(3)
Mn1–N3	2.315(2)	2.330(4)	O1-C3	1.353(3)
Mn1–N4	2.320(2)	2.320(3)	O1-C6	1.441(3)
Mn1–N5	2.333(2)	2.352(3)		
Bond	**Bond angle**	**Lliterature value Mn-H-pyane [19]**	**Bond**	**Bond angle**
N1–Mn1–N2	70.16(7)	70.2(2)	C5–C7–C8	108.5(2)
N1–Mn1–N5	69.58(8)	70.3(2)	N2–C7–C8	112.0(2)
N2–Mn1–N3	73.36(8)	74.7(2)	C1–C15–C16	111.9(2)
N3–Mn1–N4	75.08(8)	74.3(2)	N5–C15–C16	112.9(2)
N4–Mn1–N5	74.49(8)	73.7(2)	C3–O1–C6	118.0(2)
Cl1–Mn1–Cl2	172.14(3)	173.4(2) [b]		

a) Value reported for Mn–O bonds of $[Mn^{II}(H\text{-pyane})(H_2O)_2]$. b) Value reported for Mn–O bonds of $[Mn^{II}(H\text{-pyane})(H_2O)_2]$.

equatorial coordination plane, while two chlorido-ligands are coordinated in the axial positions. The OMe-pyane ligand belongs to the group of pentaazamacrocycles and therefore coordinates the manganese(II) ion in a pentadentate fashion, with a nearly perfect planar arrangement. The sum of the five chelate angles is close to 360° (362.67°), which is the ideal value for a planar structure. The Cl–Mn–Cl angle is around 172.14°, indicating a close to linear axial orientation of the chlorido-ligands. The N1–Mn1–N2 and N1–Mn1–N5 angles are about 70° and therefore smaller than the ideal 72° for perfectly planar pentadentate coordination plane. This is due to limited steric flexibility of the N2 and N5 nitrogen atoms, due to their close proximity to the sterically ridged aromatic system. The other N–Mn–N bond angles are between 73° and 75°, making up for the small angles mentioned above. This is possible due to the high flexibility of the ethylene-bridged macrocycle, connecting nitrogen atoms N2-N5.

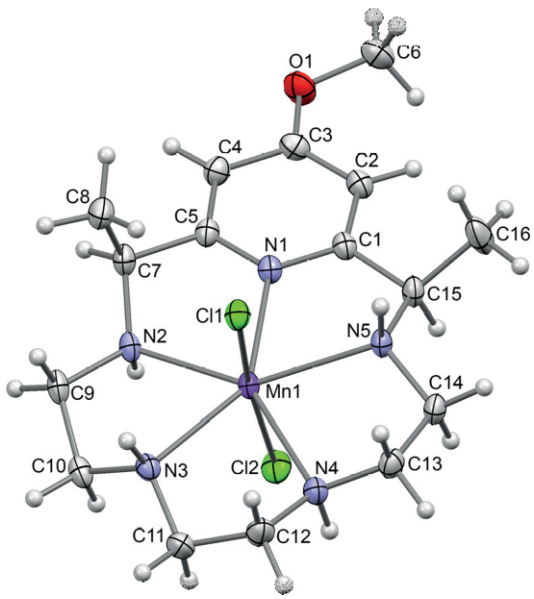

Figure 4. ORTEP model of [Mn^{II}(OMe-pyane)$(Cl)_2$]. The displacement ellipsoids represent a probability of 50 %.

Another important feature of Mn-pyane, regarding its ability to catalytically disproportionate superoxide, is the orientation of the methyl groups attached in close proximity to the pyridine subunit. This effect is best demonstrated in the case of M4040X family of analogues SOD mimetics (that possess two sterically demanding cyclohexyl units attached at the pentaaza macrocycle, resulting in various isomers), where one stereoisomer is highly active whereas a change in orientation of the methyl groups results in complete loss of SOD-like activity. Mn-pyane is less sterically demanding than the M4040X compounds and exists only as (*S*,*S*)- and (*R*,*R*)-dimethyl enantiomer with a C–CH_3 and N–H pattern that alternates up-down-up-down. Bond angles around C7 and C15 atoms are 108.5° and 111.9° respectively and close to the ideal tetrahedral angle of 109.47°. This indicates sp^3 hybridization of the C7 and C15 atoms, emerging from the imine-bond reduction of the precursor complexes. Evidence of complete imine-bond reduction to secondary amine functionalities is the C–N bond length. On average this C–N bond length is 1.472 Å, which is close to the literature value for secondary amines.[20]

Looking along the bisectrix of the crystallographic *b* and *c* axis indicates that the [Mn^{II}(OMe-pyane)$(Cl)_2$] molecules are parallel oriented, lying next to each other with an intermolecular Mn–Mn distance of 9.986 Å. Between the neighbouring CH_2 moieties we find a distance of around 3.8 Å (C–C distance). Below this ribbon of [Mn^{II}(OMe-pyane)$(Cl)_2$] complexes, antiparallel oriented and shifted by a half of molecule a second ribbon of [Mn^{II}(OMe-pyane)$(Cl)_2$] units is located. The distance between these two ribbons is again around 3.8 Å. If the structure is oriented along the *a* axis, one will recognise that both ribbons form a joined building block. These joined building blocks are forming a 45° rotated Herringbone pattern, as depicted in Figure 5

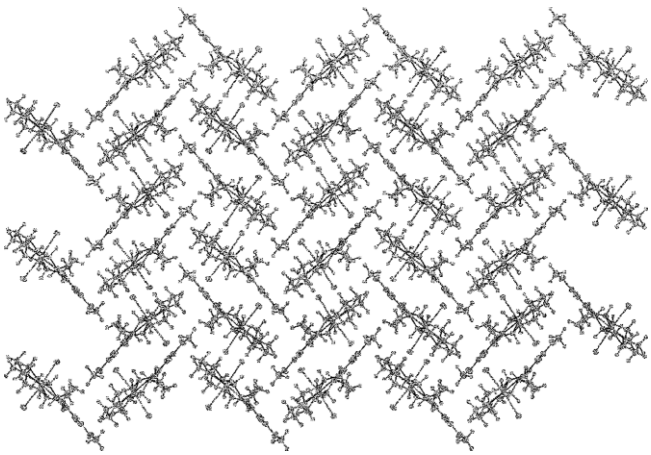

Figure 5. View along the *a* axis (hydrogen atoms are omitted for clarity).

Conclusions

In this work we have synthesized four seven-coordinate Mn complexes of the pentadentate ligand pyane substituted at 4-position of the pyridine ring. The electron withdrawing and electron donating substituents were chosen in order to vary electronic density at the central manganese atom and thus fine tune its redox potential. The series of complexes will be used in future investigations of the redox behavior of the corresponding Mn complexes and mechanistic studies of their SOD activities. The obtained results will be used to elucidate the influence of redox potentials of SOD mimetics on catalytic rate constant for the superoxide dismutation. Although measured redox potentials are usually directly correlated with the ability of the corresponding complex to redox activate a certain substrate (small molecule), researchers have to be careful when the mechanism of action is an inner-sphere electron transfer, where a direct redox-correlation is not possible[21]. The reason is that upon coordination the redox potential of a small molecule substrate is dramatically changed. Therefore, we will devote our future work to clarify this paradigm.

Acknowledgements

IIB gratefully acknowledge DFG for the Research Grant (IV 80/12–1) "Pressure Effects on Proton-Coupled Electron Transfer Reactions with Transition Metal Complexes: Towards Efficient Mechanisms for Chemical Energy Conversion". We also thank *Prof. Dr. Sjeord Harder* for the acquisition of the X-ray Diffractometer.

Keywords: Superoxide dismutase mimetic; SOD catalysis; Manganese

References

[1] C. J. Pedersen, *J. Am. Chem. Soc.* **1967**, *89*, 2495–2496.
[2] a) J. Lehn, *Angew. Chem. Int. Ed. Engl.* **1988**, *27*, 89-112.; b) C. J. Pedersen, *Angew. Chem. Int. Ed. Engl.* **1988**, *27*, 1021-1027.; c) D. J. Cram, *Angew. Chem. Int. Ed. Engl.* **1988**, *27*, 1041-1052..
[3] a) J. E. Richman, T. J. Atkins, *J. Am. Chem. Soc.* **1974**, *96*, 2268–2270; b) T. Atkins, J. Richman, W. Oettle, *Org. Synth.* **1978**, 86–86.
[4] a) D. Salvemini, C. Muscoli, D. P. Riley, S. Cuzzocrea, *Pulm. Pharmacol. Ther.* **2002**, *15*, 439–447; b) C. Muscoli, S. Cuzzocrea, D. P. Riley, J. L. Zweier, C. Thiemermann, Z.-Q. Wang, D. Salvemini, *Br. J. Pharmacol.* **2003**, *140*, 445–460; c) I. Fridovich, *Ann. N. Y. Acad. Sci.* **1999**, *893*, 13–18; d) E. R. Stadtman, *Curr. Med. Chem.* **2004**, *11*, 1105–1112.
[5] a) A. Miller, L. Que, W. Tolman, *Coord. Chem. Biosph. Geosph.* **2003**, *8*, 479–506; b) A.-F. Miller, D. Sorkin, *Comments Mol. Cell Biophys.* **1997**, *9*, 1–48.
[6] J. D. Crapo, J. M. McCord, I. Fridovich, in *Methods Enzymology*, vol. 53 (Eds.: S. Fleischer, L. Packer), Academic Press, **1978**, pp. 382–393.
[7] H. Sim Choi, J. Woo Kim, Y. N. Cha, C. Kim, *J. Immunoassay Immunochem.* **2006**, *27*, 31–44.
[8] a) I. Batinić-Haberle, A. Tovmasyan, I. Spasojević, *Bioinorg. React. Mech.* **2013**, *9*, 35–58; b) O. Iranzo, *Bioorg. Chem.* **2011**, *40*, 73–87.
[9] F. C. Friedel, D. Lieb, I. Ivanović-Burmazović, *J. Inorg. Biochem.* **2012**, *109*, 26–32.
[10] Agilent, Agilent Technologies Ltd., Yarnton, Oxfordshire, England, **2014**.
[11] G. Sheldrick, *Acta Crystallogr., Sect. A* **2008**, *64*, 112–122.
[12] O. V. Dolomanov, L. J. Bourhis, R. J. Gildea, J. A. K. Howard, H. Puschmann, *J. Appl. Crystallogr.* **2009**, *42*, 339–341.
[13] C. F. Macrae, I. J. Bruno, J. A. Chisholm, P. R. Edgington, P. McCabe, E. Pidcock, L. Rodriguez-Monge, R. Taylor, J. v. Streek, P. A. Wood, *J. Appl. Crystallogr.* **2008**, *41*, 466–470.
[14] R. Zong, H. Zhou, R. P. Thummel, *J. Org. Chem.* **2008**, *73*, 4334–4337.
[15] A. Dumont, V. Jacques, J. F. Desreux, *Tetrahedron* **2000**, *56*, 2043–2052.
[16] A. R. Katritzky, R. Murugan, *J. Chem. Soc. Perkin Trans. 2* **1987**, 1867–1869.
[17] D. Lieb, I. Kenkel, J. L. Miljković, D. Moldenhauer, N. Weber, M. R. Filipović, F. Gröhn, I. Ivanović-Burmazović, *Inorg. Chem.* **2014**, *53*, 1009–1020.
[18] K. Aston, N. Rath, A. Naik, U. Slomczynska, O. F. Schall, D. P. Riley, *Inorg. Chem.* **2001**, *40*, 1779–1789.
[19] G.-F. Liu, M. Filipović, F. W. Heinemann, I. Ivanović-Burmazović, *Inorg. Chem.* **2007**, *46*, 8825–8835.
[20] F. H. Allen, O. Kennard, D. G. Watson, L. Brammer, A. G. Orpen, R. Taylor, *J. Chem. Soc. Perkin Trans. 2* **1987**, 1–19.
[21] a) I. Ivanovic-Burmazović, R. van Eldik, *Dalton Trans.* **2008**, 5259–5275; b) I. Ivanović-Burmazović, *Adv. Inorg. Chem.* **2008**, *60*, 59–100; c) I. Ivanović-Burmazović, M. R. Filipović, *Adv. Inorg. Chem.* **2012**, *64*, 53–95.

Received: April 10, 2018
Published online: ■

Journal of Inorganic and General Chemistry
ZAAC
Zeitschrift für anorganische und allgemeine Chemie

A. Scheitler, F. Friedel, R. Puchta, C. Dücker-Benfer, I. Ivanović-Burmazović** **1–7**

Synthetic Access to Derivatized Mn-Pyane as a Redox-modulated Pool of SODm